Demixing in binary mixtures of anisometric colloids

H H Wensink and G J Vroege

Van't Hoff Laboratory for Physical and Colloid Chemistry, Debye Institute, Utrecht University, Padualaan 8, 3584 CH Utrecht, The Netherlands

E-mail: g.j.vroege@chem.uu.nl

Abstract
An overview is given of the isotropic and nematic phase behaviour in binary mixtures of hard rods or plates with different lengths or diameters within the framework of the Onsager theory. On the basis of Gaussian trial functions the relative importance of different entropic contributions in the demixing of the isotropic and nematic phases is explained for different mixtures. Modifications of this theory are discussed and new results are given for mixtures of plates differing only in diameter or thickness.

1. Introduction

The phase behaviour of anisometric particles (rods or plates) is richer than that of their spherical counterparts due to their inherent orientational degrees of freedom. Apart from a disordered, isotropic (I) fluid at low densities and a fully crystalline state at high densities, these systems may form *liquid crystals* at intermediate densities. These states are characterized by a fair degree of orientational order, whereas long-range positional order is either absent (such as in the nematic (N) state) or only partially present in one or two dimensions of the system, such as in the quasi-crystalline smectic and columnar phases, respectively.

A theoretical explanation for the formation of a nematic phase upon densification of an isotropic fluid of anisometric colloids at low densities was first provided by Onsager [1]. Although his theory focuses on monodisperse systems of thin rod-like particles, Onsager already indicated that the basic mechanism also applies essentially to thin plate-like species. The transition is a consequence of hard-core repulsions only and results directly from a competition between orientational entropy (favouring the isotropic state) and the entropy effect associated with the orientation-dependent excluded volume of two particles (which favours the nematic state).

Mixing particles with different sizes or shapes leads to an additional mixing entropy and the subtle interplay of the three entropic contributions may give rise to a rich phase behaviour. Generalizations of the Onsager theory to binary mixtures have indeed revealed aspects that are

not encountered in the monodisperse cases, such as a fractionation effect (redistributing the species among the coexisting phases) and reentrant phenomena [2–4].

The most important characteristic of these mixtures, however, is the possibility of demixing transitions in both the isotropic and nematic phases. Depending on the concentration and size ratio of the species, a homogeneous isotropic or nematic phase may split into two phases with the same symmetry but different densities and compositions. Moreover, the system may display associated triphasic equilibria, involving I–N–N or I–I–N coexistences. The demixing phenomenon was first encountered in nematic phases of rods differing only in length [5]. Later on, similar calculations based upon a generalized Onsager theory [6] revealed that the rod lengths should differ at least by a factor 3.167 in order to have a demixing of the nematic state.

In the last decade, a number of papers have appeared in which several other binary mixtures of hard anisometric colloids were treated within the Onsager approach, including mixtures of rods or plates differing only in thickness [2, 7], rods differing both in length and thickness [4, 8, 9] and rod–plate mixtures [3, 10–12]. In this paper we review existing theoretical work along with new results (mainly for plate–plate mixtures) to present an overview of the isotropic and nematic phase stability in binary mixtures of rod- and plate-like species. Here, we restrict ourselves to binary mixtures for which *only one* of the particle dimensions is unequal to both species while the other is common to all particles. In particular, we shall focus on the possibility of demixing transitions within the homogeneous isotropic and nematic phases and provide a theoretical underpinning for the associated demixing mechanisms.

2. Theoretical background

2.1. Generalized Onsager theory

To treat polydisperse systems of hard anisometric particles with total number density ρ and mole fractions x_i of species i within the second virial approximation, we start from the following expression for the Helmholtz free energy:

$$\frac{F}{Nk_{\mathrm{B}}T} \simeq \mathrm{cst} + \ln \rho - 1 + \sum_i x_i \ln x_i - \sum_i x_i \frac{\Delta S_{\mathrm{or,i}}}{Nk_{\mathrm{B}}} + \frac{1}{2}\rho g(\phi) \sum_i \sum_j x_i x_j \langle\langle v_{\mathrm{excl}} \rangle\rangle_{ij} \qquad (1)$$

where $\ln \rho - 1$ is the ideal translational entropy and $\sum_i x_i \ln x_i$ the entropy of mixing. The last two terms are the orientational entropy and the (packing) entropy related to the excluded volume (the function $g(\phi)$ is introduced for later use, but should be taken $g(\phi) = 1$ within the second virial approximation). Triangular brackets indicate (orientational) averages with respect to the distribution of species indicated by the subscript. In the remainder of this paper we will often implicitly use Gaussian trial functions [13] to describe the sharply peaked angular distributions of the particles in the nematic state. However, it will suffice to refer to these in terms of the width of the distribution for particle type i, characterized by the typical angle $\tilde{\theta}_i = \langle \theta^2 \rangle_i^{1/2}$ with the nematic director. For the orientational entropy the isotropic phase is taken as the reference state. To estimate the orientational entropy for the nematic phase just consider the number of orientational states accessible to the particles. In the isotropic phase this is proportional to the surface of the full unit sphere, 4π, whereas in the nematic phase the particles have to remain within the typical angle $\tilde{\theta}_i$ around 0 or π. For small $\tilde{\theta}_i$ these are just two circular surfaces on the unit sphere with each an approximate surface of $\pi\tilde{\theta}_i^2$. This leads to the following entropy difference ΔS_{or}

$$\begin{aligned} \Delta S_{\mathrm{or,i}} &\simeq Nk_{\mathrm{B}} \left[\ln(\#\text{ nematic states}) - \ln(\#\text{ isotropic states}) \right] \\ &\simeq Nk_{\mathrm{B}} \left[\ln(2 \times \pi\tilde{\theta}_i^2) - \ln(4\pi) \right] \end{aligned} \qquad (2)$$

$$\frac{\Delta S_{\text{or,i}}}{N k_{\text{B}}} \sim \ln(\tilde{\theta}_i^2/2) + 1. \tag{3}$$

The term +1 follows from a full calculation within the Gaussian approximation. Note that for the small widths $\tilde{\theta}_i$ of the distributions we shall encounter, $\Delta S_{\text{or,i}}$ is negative, which ought to be the case going from the random isotropic state to the more ordered nematic state. For two thin particles at mutual angle γ, we may only consider the leading order term for the excluded volume

$$\langle\langle v_{\text{excl}} \rangle\rangle_{ij} \sim \tilde{v}_{ij} \langle\langle \sin\gamma \rangle\rangle_{ij} \tag{4}$$

where $\tilde{v}_{ij} = L_i L_j (D_i + D_j)$ for thin rods while the corresponding expression for platelets reads $\tilde{v}_{ij} = \frac{\pi}{4} D_i D_j (D_i + D_j)$ in terms of the particle lengths L_i and L_j and diameters D_i and D_j. Equation (4) involves a two-particle average of $\sin\gamma$, which is always $\pi/4$ in the isotropic state, whereas in a highly ordered nematic state it is simply related to the typical angular widths of the distributions [13]:

$$\langle\langle \sin\gamma \rangle\rangle_{ij} \sim \langle\langle\gamma\rangle\rangle_{ij} \sim \tfrac{1}{2}\sqrt{\pi}(\tilde{\theta}_i^2 + \tilde{\theta}_j^2)^{1/2}. \tag{5}$$

2.1.1. Monodisperse systems. For monodisperse systems all this taken together results in a very simple expression for the Helmholtz free energy in the isotropic state:

$$\frac{F^{\text{iso}}}{N k_{\text{B}} T} \simeq \text{cst} + \ln\rho - 1 + (\pi/4)L^2 D\rho g(\phi) \simeq \text{cst}' + \ln c - 1 + cg(\phi) \tag{6}$$

where Onsager defined a dimensionless concentration $c \equiv \frac{1}{2}\langle\langle v_{\text{excl}}\rangle\rangle\rho$ related to the volume fraction ϕ via $c = l\phi$ (rods) and $l\frac{\pi}{4}\phi$ (plates). Here, l is the *aspect ratio*, defined as the ratio of the largest to the smallest dimension of the particle (i.e. for rods $l = L/D$, plates have $l = D/L$). The corresponding expression for the nematic state is found using the same ingredients:

$$\frac{F^{\text{nem}}}{N k_{\text{B}} T} \sim \text{cst}' + \ln c - 1 - \ln(\tilde{\theta}^2/2) - 1 + cg(\phi)\sqrt{\frac{8}{\pi}}\tilde{\theta} \tag{7}$$

but this expression should still be minimized with respect to the unknown parameter $\tilde{\theta}$ giving

$$\tilde{\theta} \sim \sqrt{\frac{\pi}{2}}\frac{1}{cg(\phi)} \propto \frac{1}{l\phi g(\phi)}. \tag{8}$$

Here we see that the angular distribution adapts itself such that its width is inversely proportional to the volume fraction and also inversely proportional to the aspect ratio l. If we substitute this form back into equation (7) and also refer to equation (1) a remarkable phenomenon appears for the interaction term: *the excluded volume contribution per particle, $\frac{1}{2}\langle\langle v_{\text{excl}}\rangle\rangle\rho$, in the nematic state equals the constant value of two irrespective of concentration.* This behaviour indicates that the narrowing of the distribution equation (8) exactly compensates the increasing probability of meeting other particles with increasing concentration. The final result for the free energy in the nematic state is now extremely simple:

$$\frac{F^{\text{nem}}}{N k_{\text{B}} T} \sim \text{cst}' + 3\ln c[+2\ln(g(\phi))] + \ln(4/\pi). \tag{9}$$

Due to the constancy of the excluded volume no linear contribution in c (as was found in equation (6)) is obtained. Using the thermodynamic relation $\Pi \equiv -(\partial F/\partial V)_{T,N} = k_{\text{B}} T\rho^2(\partial(F/N k_{\text{B}} T)/\partial\rho)_{T,N}$ then gives three times the ideal (Van't Hoff) osmotic pressure (setting $g(\phi) = 1$ for the time being):

$$\frac{\Pi^{\text{nem}}}{k_{\text{B}} T} \sim 3\rho. \tag{10}$$

2.1.2. Polydisperse systems. For a polydisperse system the isotropic free energy is a straightforward extension of equation (6), while the ingredients for the nematic state substituted in equation (1) give

$$\frac{F^{\text{nem}}}{Nk_{\text{B}}T} \sim \text{cst} + \ln\rho - 1 + \sum_i x_i \ln x_i - \sum_i x_i \left(2\ln(\tilde{\theta}_i/\sqrt{2}) + 1\right)$$

$$+ \frac{1}{2}\rho g(\phi)\sum_i\sum_j x_i x_j \tilde{v}_{ij}\frac{\sqrt{\pi}}{2}\sqrt{\tilde{\theta}_i^2 + \tilde{\theta}_j^2} \tag{11}$$

where $\phi = \sum_i \phi_i$ now represents the *total* volume fraction. The set of parameters $\tilde{\theta}_i$ is as yet unknown and has to be determined by simultaneous solution of the following minimization equations:

$$-\frac{2x_i}{\tilde{\theta}_i} + \rho g(\phi)x_i\sum_j x_j \tilde{v}_{ij}\frac{\sqrt{\pi}}{2}\frac{\tilde{\theta}_i}{\sqrt{\tilde{\theta}_i^2 + \tilde{\theta}_j^2}} \sim 0. \tag{12}$$

Multiplying this equation by $\tilde{\theta}_i$, summing over i and adding the resulting equation to the one obtained by interchanging i and j gives

$$\frac{1}{2}\rho g(\phi)\sum_i\sum_j x_i x_j \tilde{v}_{ij}\frac{\sqrt{\pi}}{2}\sqrt{\tilde{\theta}_i^2 + \tilde{\theta}_j^2} \sim 2. \tag{13}$$

Comparing this result to equation (11) we see that it is just the excluded-volume term within the free energy, so that we can state: *the excluded-volume contribution per particle in the nematic state equals the constant value of two irrespective of concentration or polydispersity* [14]. Although solving equation (12) for the set $\{\tilde{\theta}_i\}$ is only possible numerically, it can be easily verified that an inverse proportionality to $(\rho g(\phi))$ is retained for every $\tilde{\theta}_i$ [15]. Using this information in equation (11) reveals the following structure for the free energy in the nematic state:

$$\frac{F^{\text{nem}}}{Nk_{\text{B}}T} \sim \text{cst} + 3\ln\rho[+2\ln(g(\phi))] + \mathcal{F}(\{x_i\}) \tag{14}$$

where concentration (ρ) and composition ($\{x_i\}$) dependence are in separate terms. The former leads again to the quasi-ideal osmotic pressure equation (10) (considering that $g(\phi) = 1$), completely independent of the composition of the nematic state. The latter also contains a non-trivial contribution originating from the orientational entropy in equation (11). Consequently the chemical potentials of species i, obtained from $\mu_i = (\partial F/\partial N_i)_{N_{j\neq i},V,T}$ have a non-trivial composition dependence, which may drive phase separations as described later.

2.2. Parsons–Lee approach

To go beyond the second virial approximation the so-called *Parsons–Lee method* [16–18] is often applied, which essentially rescales the total excluded volume of the system to that of a hard-sphere system and then uses the semi-empirical Carnahan–Starling form for hard spheres as a volume-fraction dependence. This method works quite well for monodisperse rods [17–19] and has also been successfully applied to mixtures of rods and plates [3, 11]. In its simplest form it corresponds to using the following form for the function $g(\phi)$ in the considerations sketched above:

$$g(\phi) \equiv \frac{1 - (3/4)\phi}{(1 - \phi)^2}. \tag{15}$$

For small volume fractions this reduces to $g(\phi) = 1$ and we recover the second virial approximation. Looking back to the previous section we see that most conclusions remain valid (except for somewhat more complicated ϕ dependences).

2.3. Gaussian approximation versus formal approach

A formal approach to the minimization of the free energy in the nematic state follows from realizing that there is a *continuous* spread of angles θ_i of particle type i with the director along the interval $0 < \theta_i < \pi$. The orientational averages in the free energy equation (1) can be rewritten in terms of continuous orientational distribution functions (ODFs). Thermodynamically consistent solutions for these functions are obtained by performing functional differentiations with respect to the ODFs and solving the resulting minimization equations. These equations constitute a coupled set of nonlinear integral equations which can be solved only by applying appropriate numerical techniques [20]. In the Gaussian approximation implicitly used above it is assumed that the ODFs obey a *prescribed* Gaussian form ($\sim \tilde{\theta}_i^{-2} \exp[-\theta_i^2/\tilde{\theta}_i^2]$) and the free energy minimization is then carried out by a simple differentiation with respect to the typical angle $\tilde{\theta}_i$. Unlike the formal approach, the Gaussian approximation allows us to obtain explicit asymptotic expressions for the orientational and packing entropies in the nematic state, at least for the monodisperse case [21].

Although the Gaussian ODF does not qualify as an exact thermodynamic equilibrium ODF it shows the correct high-density scaling behaviour such that the approximation is expected to be satisfactory for strongly aligned nematic states [22]. As to the binary mixtures to be considered in the following we may intuitively expect the Gaussian approach to work particularly well for mixtures with extreme size ratios where the degree of alignment of both species is usually very strong (due to their size difference).

2.4. Phase stability in binary mixtures

Let us now focus on binary mixtures of hard particles with total number density ρ and mole fraction x (usually denoting the fraction of the *largest* species) and briefly sketch the conditions for phase equilibria. Two phases (e.g. isotropic I and nematic N) are in equilibrium when the osmotic pressure and chemical potentials of the components, obtained by taking appropriate partial derivatives of the free energy, have the same value in both phases. After the coexistence equations have been solved we can combine the results in a phase diagram. In this paper, we will use a field-density (Π–x) representation in terms of the osmotic coexistence pressure plotted versus the mole fraction of the coexisting phases. In this representation, coexisting state points are given by horizontal tie lines. For comparison with experimental phase diagrams, however, it is often useful to employ a density–density (ϕ_1–ϕ_2) representation involving the species volume fractions in the separate phases [6, 23]. We will not use this representation here.

The next step is to verify the thermodynamic stability of the isotropic and nematic phases with respect to a demixing into two phases with the same symmetry. A convenient thermodynamic variable to analyse the *local* stability of a homogeneous phase with respect to infinitesimal fluctuations in the density and composition (at constant osmotic pressure) is the Gibbs free energy $\beta G/N$ which can be obtained from the Helmholtz free energy by a Laplace transform: $G/N = F/N + \rho^{-1}\Pi$. The condition for local stability then follows from the second derivative of the Gibbs free energy with respect to the mole fraction [24, 25]:

$$\left(\frac{\partial^2 \tilde{g}}{\partial x^2}\right)_{T,\Pi} > 0 \tag{16}$$

at constant temperature T and osmotic pressure Π. In practice, it is usually more convenient to rewrite this explicitly in terms of derivatives of the Helmholtz free energy with respect to

density and composition:

$$\left(\frac{\partial^2 \tilde{f}}{\partial x^2}\right)_{T,\rho} - \rho\left(\frac{\partial^2 \tilde{f}}{\partial x \partial \rho}\right)^2 \left[2\frac{\partial \tilde{f}}{\partial \rho} + \rho\frac{\partial^2 \tilde{f}}{\partial \rho^2}\right]_{T,x}^{-1} > 0 \tag{17}$$

where $\tilde{g} = G/Nk_\mathrm{B}T$ and $\tilde{f} = F/Nk_\mathrm{B}T$ denote *intensive* free energies. The limit of stability of the mixed state is given by $(\partial^2 \tilde{g}/\partial x^2)_{T,\Pi} = 0$. The solutions $\rho_\mathrm{s}(x)$ of this equation represent the so-called spinodal curve. The corresponding spinodal pressure Π_s can be obtained by inserting $\rho = \rho_\mathrm{s}(x)$ into the osmotic pressure. The critical point (Π^*, x^*) of the demixing transition is then obtained from the condition $\mathrm{d}\Pi_\mathrm{s}(x)/\mathrm{d}x = 0$. Corresponding demixing binodals can be computed in the same way as described above by requiring equal osmotic pressure and chemical potentials of both components in the demixed phases.

3. Isotropic–nematic fractionation phenomena

For the sake of clarity let us now define the following binary mixtures. R-I: rods with different lengths (L) but equal thickness (D), R-II: rods with different diameters but equal length, and likewise for the platelets, P-I: platelets with equal thickness (L) differing in diameter (D) and P-II: platelets with equal diameter but different thickness. To investigate the behaviour of the latter we need to include the next order (thickness dependent) contribution to the excluded volume of two platelets equation (4) [7]. The reason for this is that the plate's thickness does not enter into the leading order contribution of the excluded volume $\tilde{v}_{ij}$, so that retaining the leading term only does not allow discrimination between plates differing only in thickness.

In figure 1 we show two phase diagrams which are representative for binary mixtures of platelets differing in thickness or diameter (i.e. cases P-I and P-II). From the osmotic pressure representations we can immediately infer a strong repartitioning of the species among the coexisting isotropic and nematic phases, i.e. the different phases are markedly enriched in either the large or the small species. However, the two scenarios depicted in figure 1 are quite distinct. For mixture P-I the largest species appear to preferentially occupy the nematic phase whereas in the other case the large platelets accumulate in the isotropic phase. Fractionation in binary mixtures of rods (both R-I and R-II) occurs in a way similar to that of plates with different diameters (P-I) as sketched in figure 1(a) with a preference of the longer/thicker rods for the nematic phase [2, 26].

The anomalous fractionation behaviour of platelet mixture P-II may lead to an *inversion of densities* of the isotropic and nematic phases. Consequently this may give an isotropic lower phase in coexistence with a nematic upper phase in a test tube as recently observed experimentally [27]. This behaviour can easily be rationalized from figure 1(a). Although the isotropic phase always has a lower number density than the nematic phase, its *mass* density, which also depends upon the average particle size in the phase, may become higher than that of the nematic phase due to fractionation, the biggest particles migrating into the isotropic phase.

4. Demixing of the isotropic and nematic phases

4.1. Symmetry-conserved nematic–nematic demixing

As we can see from the phase diagrams depicted in figure 1, a homogeneous nematic system may under certain conditions demix into two nematic phases with the same uniaxial nematic symmetry but with different number densities and compositions. For all four mixtures considered in this paper, this demixing transition can occur if the corresponding length or
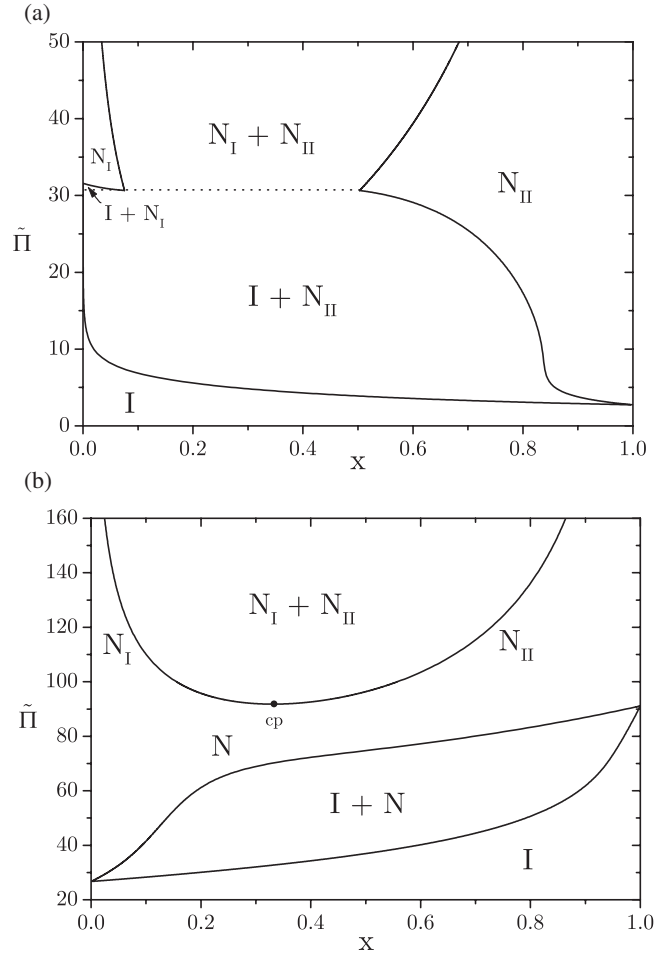
(a)

(b)

Figure 1. Phase diagrams in terms of osmotic pressure $\tilde{\Pi} = (1/2)\langle\langle v_{\text{excl}}\rangle\rangle_{11}^{\text{iso}}\Pi/k_BT$ plotted versus the mole fraction of the largest species $x = x_2$ obtained from the Onsager theory using Parsons–Lee rescaling. (a) Case P-I: mixture of platelets with equal thickness but different diameters ($L_1 = L_2$, $l_1 = 10$, $l_2 = 20$). The dotted line represents an I–N_I–N_{II} triple line. (b) Case P-II: binary mixture of thin and thick hard platelets with equal diameter ($D_1 = D_2$, $l_1 = 9$, $l_2 = 4$).

thickness ratio exceeds some threshold value. However, the interplay of the different entropic contributions involved can lead to distinctly different demixing mechanisms for these mixtures.

Judging from the structure of the nematic free energy equation (11), it is obvious that the demixing must be driven by a competition between mixing, orientation and packing (i.e. excluded-volume) entropy. However, since the latter contribution is a constant independent of the composition for all cases (except for the plates with bidisperse thickness, P-II) it is clear that the excluded-volume effect plays no role and that the demixing involves a balance between mixing and orientational entropy. In the case of rods with length bidispersity (R-I) the orientational entropy of the *short* rods favours demixing because of the strong alignment the long rods impose on the short in the mixed nematic phase [6]. Demixing occurs when the gain of orientational entropy outweighs the simultaneous loss of mixing entropy. A similar scenario applies to the other mixtures R-II and P-I, while case P-II is an exception because there

the demixing is essentially driven by a competition between mixing and the excess packing entropy due to the plates' thickness (rather than their orientational entropy, as shown explicitly in [7]).

The underlying mechanism may also have important implications for the topology of the nematic–nematic coexistence region. In particular, if the packing entropy is irrelevant all binodals can be shown to be completely independent of concentration and osmotic pressure[1]. This is easily understood by considering the Gibbs free energy of the nematic phase. Applying the appropriate Laplace transform of equation (14) and using the osmotic pressure equation (10) gives

$$\tilde{g}^{\text{nem}}(\Pi, x) \sim \text{cst} + 3\ln(\Pi/3) + \mathcal{F}(x, q). \tag{18}$$

Since the first terms are trivial contributions independent of the mole fraction, it is clear that the last contribution is solely responsible for the demixing and that the presence of an instability is only determined by the size ratio q. This means that the demixing binodals do *not* depend upon the concentration or the osmotic pressure of the nematic phase. Consequently, in a Π–x representation, all binodals must be straight vertical lines [6]. The *threshold* value for q above which an instability occurs was found at $q = 3.167$ for rods of type R-I [6], whereas the platelets of type P-I demix at considerably lower size ratios $q > 1.753$. Based on similar calculations, Hemmer [8] found that for the case R-II a diameter ratio larger than 4.258 is required.

As mentioned already, mixtures of thin and thick platelets (P-II) are governed by a different demixing scenario. There, the excluded-volume contribution (more precisely, the thickness-dependent correction term) is responsible for the demixing. The packing contribution of the Gibbs free energy (which favours demixing) for the case P-II reads

$$\tilde{g}^{\text{nem}}_{\text{excl}} = 2 + 8\phi = 2 + \frac{32}{\pi} c(\Pi, x) \sum_{i=1,2} x_i \frac{L_i}{D} \tag{19}$$

where the concentration $c(\Pi, x)$ follows from inverting the equation of state [7]. Due to its concentration dependence the latter term in equation (19) will always outweigh the mixing contribution at sufficiently high pressures, irrespective of the size ratio. Therefore, there is no threshold value in these mixtures and demixing occurs at any size ratio. However, in order for the critical pressure to attain physically acceptable values it is required that the thickness ratio is larger than three [7].

To assess the effect of Parsons–Lee rescaling on the shape of the demixing binodals we may analyse its additional contribution to the Gibbs free energy equation (18). The osmotic pressure of the nematic state within the Parsons–Lee approach becomes

$$\frac{\Pi^{\text{nem}}}{k_{\text{B}}T} \sim c \left[3 + 2\frac{\partial \ln g(\phi(x, c))}{\partial \ln \phi(x, c)} \right]. \tag{20}$$

Inverting the pressure now yields a non-trivial mole-fraction dependence of the concentration $c(\Pi, x)$ (compared to a simple $c(\Pi) = \Pi/3$ for the case $g(\phi) = 1$). This implies that all binodals become implicitly dependent upon the osmotic pressure so that they no longer form straight lines in a Π–x phase representation, as we see in figure 1. As to the Gibbs free energy, the trivial second term in equation (18) should now be replaced by the following non-trivial contribution

$$\tilde{g}^{\text{P}-\text{L}}(\Pi, x) \sim 3\ln c\,[\Pi(x)] + 2\ln g(x, c\,[\Pi(x)]). \tag{21}$$

To verify whether this contribution stabilizes or destabilizes the homogeneous nematic state we must know the sign of its second order derivative with respect to the mole fraction.

---

[1] Formally, this conclusion is only valid within the Gaussian trial function Ansatz we implicitly use here.

This calculation can only be done in a numerical way since it is not possible to invert the osmotic pressure equation (20) analytically. It turns out that $(\partial^2 \tilde{g}^{P-L}/\partial x^2)$ is generally positive indicating that the correction due to the Parson–Lee rescaling always *favours the mixed state*. Consequently the critical values mentioned above need to be adapted slightly due to the rescaling. An interesting manifestation of the stabilizing effect of the Parson–Lee approach is the possibility of the demixing binodals closing off at a lower critical point. This would give a scenario similar to the one shown in figure 1(b) for the case P-II; although the size ratio is larger than the threshold value the nematic–nematic two-phase region only opens up when the pressure exceeds a certain value. Note that this scenario is not encountered without the Parsons–Lee rescaling since the binodals then run vertically and therefore cannot meet in a critical point. At higher size ratios, the critical point shifts to lower values of the pressures and the nematic–nematic demixing region eventually overlaps with the isotropic–nematic region. This gives rise to an isotropic–nematic–nematic triple equilibrium, according to the scenario shown in figure 1(a).

Calculations based upon the formal minimization approach (see section 2.3) reveal the possibility of an *upper* critical or consolute point which marks the closing of the nematic–nematic region at high pressures and the re-entrance of the homogeneous nematic state. These have been found in mixtures of rods with different lengths (R-I) [28] (albeit in an extremely small q interval at low size ratios) and in mixtures of thin and thick hard rods (R-II) [2]. The fact that this phenomenon is not observed in the Gaussian approach is probably related to the fact that the ODFs are not represented by their true equilibrium form. However, in both cases the consolute points disappear at higher size ratios such that the high-q scenarios obtained within the formal approach are consistent with the one sketched for the Gaussian approximation in figure 1(a).

4.2. Isotropic–isotropic demixing

Contrary to the nematic phase, a demixing of the isotropic phase is less common. So far, such an instability was only found in binary mixtures of thin and thick rods (R-II) [2, 9, 25]. However, extending the simple spinodal analysis from [25] it can be easily verified that a similar demixing may take place in mixtures of platelets, both for P-I and P-II. Consider the free energy in the isotropic state

$$\tilde{f}^{\text{iso}} \sim \text{cst} + \ln \rho - 1 + \sum_{i=1,2} x_i \ln x_i + \tfrac{1}{2}\rho g(\phi) B_2^{\text{iso}} \tag{22}$$

with B_2^{iso} the excluded-volume dependent second virial coefficient:

$$B_2^{\text{iso}} = \frac{\pi}{4}\left((1-x)^2\tilde{v}_{11} + 2x(1-x)\tilde{v}_{12} + x^2\tilde{v}_{22}\right). \tag{23}$$

Inserting this into equation (17) (setting $g(\phi) = 1$ for simplicity) and some rearrangements lead to the following stability condition [25]:

$$1 + \rho\frac{\pi}{4}\left((1-x)\tilde{v}_{11} + x\tilde{v}_{22}\right) - \left(\rho\frac{\pi}{4}\right)^2 x(1-x)\Delta > 0. \tag{24}$$

To arrive at equation (24) it is implicitly used that the system also fulfils the criterion for *mechanical* stability $(\partial^2 \tilde{f}/\partial v^2)_x > 0$, where $v = 1/\rho$ [24]. A demixing instability is only possible if $\Delta \equiv \tilde{v}_{12}^2 - \tilde{v}_{11}\tilde{v}_{22} > 0$ since only then is the condition equation (24) no longer satisfied for all $\rho > 0$. Substituting corresponding expressions for $\tilde{v}_{ij}$ (including the thickness dependent contribution for the case P-II) yields $\Delta > 0$ for all cases except for R-I, for which $\Delta = 0$. Hence, an isotropic–isotropic demixing may in principle be expected in all mixtures, except in binary systems of rods differing only in length.
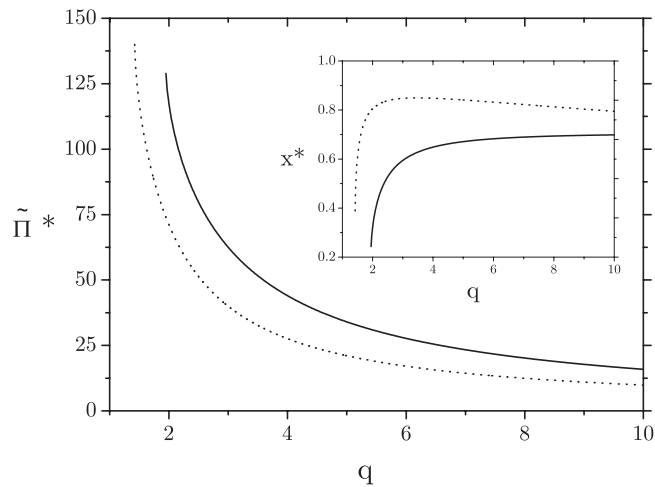
Figure 2. Locus of the isotropic–isotropic critical point, in terms of the critical pressure $\tilde{\Pi}^*$ and mole fraction x^* (inset), for binary plate mixtures P-I (solid curve, $q = D_2/D_1$) and P-II (dotted curve, $q = L_2/L_1$). Results are based on the Onsager–Parsons–Lee free energy using $l_1 = L/D_1 = L_1/D = 0.05$.

Explicit results can be obtained by calculating spinodal curves (and their corresponding critical point) from equation (17) as a function of the size ratio. To illustrate this we have plotted in figure 2 the evolution of the isotropic–isotropic critical point for the binary plate mixtures P-I and P-II. Physical solutions are found for size ratios $q = D_2/D_1 > 1.95$ (P-I) and $q = L_2/L_1 > 1.42$ (P-II). However, considering the high osmotic pressures at low size ratios it is evident that the isotropic state (and therefore its demixing) will initially be *metastable* with respect to a transition to the nematic state. In order to estimate the minimum size ratio required for having *stable* demixing transitions we should compare the critical pressure in figure 2 with the maximum coexistence pressure pertaining to the isotropic–nematic transition. From this we obtain that $q > 7.4$ for P-I and $q > 2.85$ for P-II. Note that these values represent *lower* bounds to the metastable–stable transition and the exact transitions generally occur at higher size ratios. For the case R-II, the transition was predicted at $q > 8$ [2]. The fact that a demixing of the isotropic phase requires a considerably larger size ratio than the nematic phase is not surprising because the orientation entropy, which usually favours demixing, is not present in the isotropic state. Consequently, the demixing must be solely accomplished by excluded-volume effects, in particular the unfavourable excluded volumes between unlike particles, as we can infer from the condition $\Delta > 0$.

Finally, we remark that the phase behaviour of platelets (P-I and P-II) can be surprisingly rich, with a possibility of both N–N and I–I two phase equilibria and their associated I–N_I–N_{II} and I_I–I_{II}–N triple equilibria, without having to go to extreme size ratios.

5. Nematic–nematic demixing in rod–plate mixtures; symmetry-broken demixing

In the systems discussed so far we have restricted ourselves to nematic phases with a common uniaxial symmetry. However, when mixing particles with distinctly different shapes, e.g. rods and plates, several nematic phases with different symmetries may come into play and the phase behaviour of these systems can become considerably more complicated. For rod–plate mixtures, we may consider three types of nematic phase, two uniaxial ones (usually denoted by
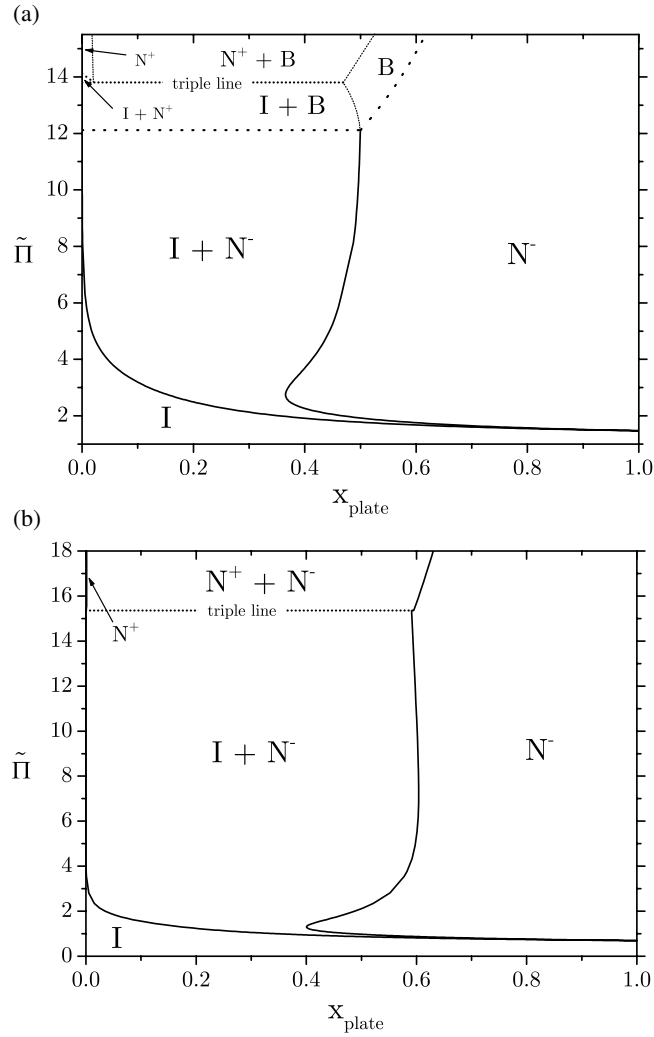
(a)

(b)

Figure 3. (a) Phase diagram of an asymmetric rod–plate mixture in the osmotic pressure–composition plane obtained from the Onsager theory ($g(\phi) = 1$). The aspect ratio of the rods and plates are, $l_R = 15$ and $l_P = 14$, respectively. The rods and plates have equal thickness ($D_R = L_P$). The dotted line indicates a continuous transition from a uniaxial (N^-) to the biaxial (B) nematic symmetry. Thin dotted lines are sketched lines indicating the topology at high pressure. (b) Same for $l_R = 15$ and $l_P = 18$ and equal thickness.

N^+ and N^-) and a biaxial B phase. The uniaxial phases are characterized by *polar* orientation of one species (i.e. alignment along the nematic director) while the other is oriented in a *planar* fashion (alignment of its symmetry axis in the plane normal to the director). In the biaxial case both species exhibit polar orientation along mutually perpendicular nematic directors. The relative stability of the different nematic symmetries was analysed for various mixtures and approximations within the Onsager theory [3, 10–12, 29, 30]. Special attention was given to the stability of the biaxial nematic phase with respect to a demixing into the uniaxial nematic ones (i.e. the rod-rich N^+ and plate-rich N^- phases).

This issue can be nicely illustrated by considering so-called *asymmetric* mixtures, characterized by a large excluded volume ratio between the like particles, such that

$\langle\langle v_{\mathrm{excl}}\rangle\rangle_{\mathrm{PP}} \gg \langle\langle v_{\mathrm{excl}}\rangle\rangle_{\mathrm{RR}}$. These mixtures are also interesting because they closely resemble the colloidal rod–plate mixtures studied experimentally by Van der Kooij *et al* [31, 32]. An example of the subtle phase stability in these mixtures is depicted in figure 3. The phase diagrams are based upon calculations within the second virial approach ($g(\phi) = 1$) employing formal free energy minimizations [33]. Figure 3(a) shows that all nematic symmetries are present but their (meta)stability is strongly dependent upon the osmotic pressure. At low pressures the phase behaviour is dominated by the isotropic phase in coexistence with the plate-dominated N⁻ phase. When the pressure $\tilde{\Pi}$ exceeds about 12 the symmetry of the latter changes *continuously* to a biaxial one. At the triple pressure, a second nematic phase comes into play, the uniaxial rod-rich nematic phase N⁺. Finally, the high-density regime is characterized by coexistence between the uniaxial N⁺ and biaxial nematic phases. Figure 3(b) shows a similar diagram for a mixture with enhanced asymmetry (i.e. the aspect ratio of the plates is increased, while that of the rods is fixed at 15). In this case, the biaxial phase is *metastable* with respect to a demixing into the two uniaxial nematic phases. Note that the phase diagram now resembles the one depicted in figure 1(a).

One of the key issues left open for future investigation is the question how the stability of the biaxial nematic phase depends upon the effects of multi-particle correlations which are not taken into account in the Onsager description. Recent calculations by Varga *et al* [29] indicate that the stability depends quite sensitively on the effect of Parsons–Lee rescaling and also on the corrections due to end effects in the excluded volume equation (4) (which correct for the particles' finite thicknesses). However, resolving this issue in a correct way requires a systematic direct inclusion of many-body excluded volume terms into the free energy, rather than indirectly accounting for these via the Parsons–Lee rescaling of the two-particle excluded volumes. Since it is impossible to carry this out in a theoretical study, we believe it to be a future challenge for computer simulators and experimentalists to verify what is really observed in these mixtures.

6. Final remarks

In this paper we have not treated the possibility of phase transitions from the nematic state to high-density liquid crystal symmetries with (partial) positional order, such as smectic and columnar phases. Since these phases are expected to appear in the high-pressure regime of the phase diagram, instabilities of the nematic state towards smectic/columnar ordering may interrupt the topology of the nematic–nematic demixing regimes in figures 1 and 3. So far such instabilities have only been analysed theoretically for a perfectly aligned nematic state of short and long rods (R-I) and thick and thin rods (R-II) [25]. There it was found that under certain conditions the demixing of the nematic phase is indeed pre-empted by transitions to smectic or columnar states. Recent simulations on mixtures of hard rods and plates also indicate that the nematic phases (and hence their possible demixing transitions) are strongly impeded by phase transitions to other phases possessing partial long-range order of one of the species [34, 35]. Clearly, further research is required to map the details of the phase behaviour of mixed hard anisometric particles at high densities.

References

[1] Onsager L 1949 *Ann. New York Acad. Sci.* **51** 627
[2] van Roij R, Mulder B and Dijkstra M 1998 *Physica* A **261** 374
[3] Wensink H H, Vroege G J and Lekkerkerker H N W 2001 *J. Chem. Phys.* **115** 7319
[4] Varga S, Galindo A and Jackson G 2003 *Mol. Phys.* **101** 817

[5] Birshtein T M, Kolegov B I and Pryamitsin V A 1988 *Polym. Sci. USSR* **30** 316
[6] Vroege G J and Lekkerkerker H N W 1993 *J. Phys. Chem.* **97** 3601
[7] Wensink H H, Vroege G J and Lekkerkerker H N W 2001 *J. Phys. Chem.* B **105** 10610
[8] Hemmer P C 1999 *Mol. Phys.* **96** 1153
[9] Hemmer P C 2000 *J. Stat. Phys.* **100** 3
[10] Chrzanowska A 1998 *Phys. Rev.* E **58** 3229
[11] Camp P J and Allen M P 1996 *Physica* A **229** 410
[12] Varga S, Galindo A and Jackson G 2002 *Phys. Rev.* E **66** 011707
[13] Odijk T and Lekkerkerker H N W 1985 *J. Phys. Chem.* **89** 2090
[14] Odijk T 1986 *Liq. Cryst.* **1** 97
[15] Wensink H H and Vroege G J 2003 *J. Chem. Phys.* **119** 6868
[16] Parsons J D 1979 *Phys. Rev.* A **19** 1225
[17] Lee S D 1987 *J. Chem. Phys.* **87** 4972
[18] Lee S D 1989 *J. Chem. Phys.* **89** 7036
[19] Camp P J, Mason C P, Allen M P, Khare A A and Kofke D A 1996 *J. Chem. Phys.* **105** 2837
[20] Herzfeld J, Berger A E and Wingate J W 1984 *Macromolecules* **17** 1718
[21] Vroege G J and Lekkerkerker H N W 1992 *Rep. Prog. Phys.* **55** 1241
[22] van Roij R and Mulder B 1996 *J. Chem. Phys.* **105** 11237
[23] DeHoff R T 1993 *Thermodynamics in Material Science* (New York: McGraw-Hill)
[24] Callen H B 1985 *Thermodynamics and an Introduction to Thermostatistics* (New York: Wiley)
[25] van Roij R and Mulder B 1996 *Phys. Rev.* E **54** 6430
[26] Lekkerkerker H N W, Coulon Ph, van der Hagen R and Deblieck R 1984 *J. Chem. Phys.* **80** 3427
[27] van der Kooij F M, van der Beek D and Lekkerkerker H N W 2001 *J. Phys. Chem.* B **105** 1696
[28] Varga S and Szalai I 2000 *Phys. Chem. Chem. Phys.* **2** 1955
[29] Varga S, Galindo A and Jackson G 2002 *J. Chem. Phys.* **117** 10412
[30] Stroobants A and Lekkerkerker H N W 1984 *J. Phys. Chem.* **88** 3669
[31] van der Kooij F M and Lekkerkerker H N W 2000 *Langmuir* **16** 10144
[32] van der Kooij F M and Lekkerkerker H N W 2000 *Phys. Rev. Lett.* **84** 781
[33] Wensink H H, Vroege G J and Lekkerkerker H N W 2002 *Phys. Rev.* E **66** 041704
[34] Galindo A, Jackson G and Photinos D J 2000 *Chem. Phys. Lett.* **325** 631
[35] Galindo A, Haslam A J, Varga S, Jackson G, Vanakaras A G, Photinos D J and Dunmur D A 2003 *J. Chem. Phys.* **119** 5216